Research Square

Preprints are preliminary reports that have not undergone peer review.
They should not be considered conclusive, used to inform clinical practice,
or referenced by the media as validated information.

Novel (R)-Camphor-Derived Thiosemicarbazones and Thiazolidinones as Potential Antiparasitic Agents: Synthesis, Biological Evaluation, Molecular Docking, ADMET, and DFT Studies

Abdellah N'ait Ousidi
Laboratory of Molecular Chemistry, unit of Organic Synthesis and Molecular Physico-Chemistry, Department of Chemistry, Faculty of Sciences Semlalia, Université Cadi Ayyad, Marrakech, Morocco

Abdoullah Bimoussa
bimoussa_@hotmail.com

Bioorganic Chemistry Team, Department of Chemistry, Faculty of Sciences, Chouaïb Doukkali University, P.O. Box 24, 24000 El Jadida, Morocco.

Mohammed Loubidi
Institut de Chimie Organique et Analytique ICOA, Université d'Orléans-Pôle de Chimie, UMR CNRS 7311, Rue de Chartres-BP 6759, 45067 Orléans Cedex 2, France

Sabine Berteina-Raboin
Institut de Chimie Organique et Analytique ICOA, Université d'Orléans-Pôle de Chimie, UMR CNRS 7311, Rue de Chartres-BP 6759, 45067 Orléans Cedex 2, France

Syeda Abida Ejaz
Department of Pharmaceutical Chemistry, The Islamia University of Bahawalpur, Bahawalpur, 63100, Pakistan.

Hafiz Muhammad Attaullah
Department of Pharmaceutical Chemistry, The Islamia University of Bahawalpur, Bahawalpur, 63100, Pakistan.

Ibrahim S. Al Nasr
Department of Biology, College of Science, Qassim University, Qassim 51452, Saudi Arabia

Waleed S. Koko
Department of Biology, College of Science, Qassim University, Qassim 51452, Saudi Arabia

Tariq A. Khan
Department of Basic Health Sciences, College of Applied Medical Sciences, Qassim University, Qassim 51452, Saudi Arabia

Rabiaa Fdil
Bioorganic Chemistry Team, Department of Chemistry, Faculty of Sciences, Chouaïb Doukkali University, P.O. Box 24, 24000 El Jadida, Morocco.

Bernhard Biersack
Organic Chemistry Laboratory, University of Bayreuth, Universitätsstrasse 30, 95447 Bayreuth, Germany.
Aziz Auhmani
Laboratory of Molecular Chemistry, unit of Organic Synthesis and Molecular Physico-Chemistry, Department of Chemistry, Faculty of Sciences Semlalia, Université Cadi Ayyad, Marrakech, Morocco
Moulay Youssef Ait Itto
Laboratory of Molecular Chemistry, unit of Organic Synthesis and Molecular Physico-Chemistry, Department of Chemistry, Faculty of Sciences Semlalia, Université Cadi Ayyad, Marrakech, Morocco

---

Research Article

Keywords: (R)-Camphor, Thiazolidinone derivatives, Leishmania major, Toxoplasma gondii, DFT, Molecular docking

Posted Date: November 16th, 2026

DOI: https://doi.org/10.21203/rs.3.rs-11331699/v1

License: This work is licensed under a Creative Commons Attribution 4.0 International License.
Read Full License

Additional Declarations: No competing interests reported.

Novel (R)-Camphor-Derived Thiosemicarbazones and Thiazolidinones as Potential Antiparasitic Agents: Synthesis, Biological Evaluation, Molecular Docking, ADMET, and DFT Studies

Abdellah N'ait Ousidi [1], Abdoullah Bimoussa [1, 2, *], Mohammed Loubidi [3], Sabine Berteina-Raboin [3], Syeda Abida Ejaz [4], Hafiz Muhammad Attaullah [4], Ibrahim S. Al Nasr [5, *], Waleed S. Koko [5], Tariq A. Khan [6,], Rabiaa Fdil [2], Bernhard Biersack [7], Aziz Auhmani [1], Moulay Youssef Ait Itto [1, *]

[1-]Laboratory of Molecular Chemistry, unit of Organic Synthesis and Molecular Physico-Chemistry, Department of Chemistry, Faculty of Sciences Semlalia, Université Cadi Ayyad, Marrakech, Morocco
[2-]Bioorganic Chemistry Team, Department of Chemistry, Faculty of Sciences, Chouaïb Doukkali University, P.O. Box 24, 24000 El Jadida, Morocco.
[3-]Institut de Chimie Organique et Analytique ICOA, Université d'Orléans-Pôle de Chimie, UMR CNRS 7311, Rue de Chartres-BP 6759, 45067 Orléans Cedex 2, France
[4-]Department of Pharmaceutical Chemistry, The Islamia University of Bahawalpur, Bahawalpur, 63100, Pakistan.
[5-]Department of Biology, College of Science, Qassim University, Qassim 51452, Saudi Arabia
[6-]Department of Basic Health Sciences, College of Applied Medical Sciences, Qassim University, Qassim 51452, Saudi Arabia
[7-]Organic Chemistry Laboratory, University of Bayreuth, Universitätsstrasse 30, 95447 Bayreuth, Germany.

*Corresponding authors: E-mail:
A. Bimoussa: bimoussa_@hotmail.com.
My Youssef Ait Itto: aititto@uca.ma
Ibrahim S. Al Nasr: insar@qu.edu.sa

Abstract:

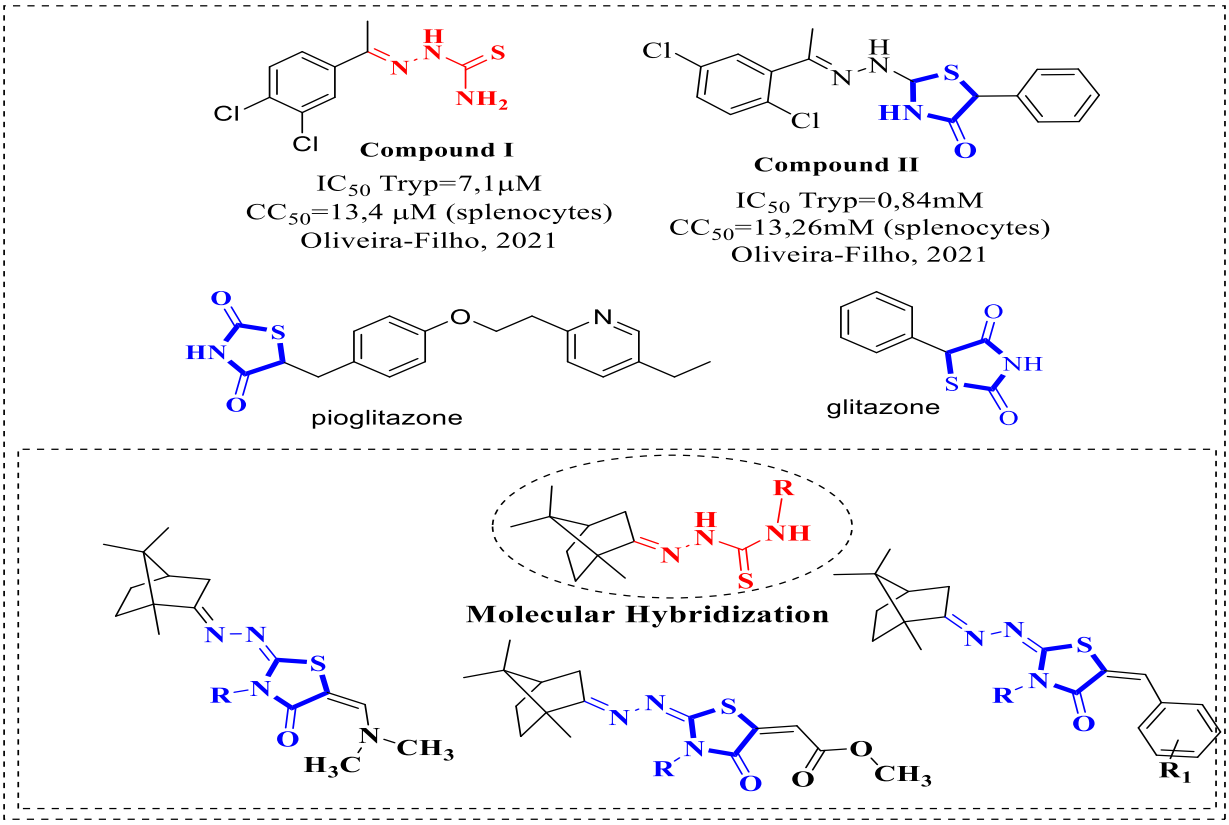
This study reports the synthesis of a novel series of (R)-camphor-based thiosemicarbazones and thiazolidinones derivatives. We obtained the compounds through heterocyclization and Knoevenagel-type condensation reactions, and characterized them by HRMS and NMR spectroscopy. Several derivatives exhibited promising *in vitro* antiparasitic activity against *Leishmania major* promastigotes and amastigotes, as well as *Toxoplasma gondii* tachyzoites. Compound 1 showed activity against *L. major* amastigotes and promastigotes, with EC_{50} values of 0.5 and 11.9 µg/mL, respectively. Compounds **2a, 6a, 6b, 5a,** and **3a–c** were active against *L. major* promastigotes (EC_{50} < 10 µg/mL), while **4a–c** and **5a–c** exhibited antitoxoplasmal activity (EC_{50} < 11 µg/mL). Molecular docking identified **2a, 3a**, and **3b** as compounds with multiple interactions with the active site of trypanothione reductase and N-myristoyltransferase. We performed DFT calculations at the B3LYP/6-311++G(d,p) level to investigate their optimized geometries and HOMO–LUMO gaps, and used SwissADME to assess their pharmacokinetic properties. The results identify selected (R)-camphor-derived thiazolidinones as promising starting points for further antiparasitic investigation.

Keywords: (R)-Camphor, Thiazolidinone derivatives, *Leishmania major*, *Toxoplasma gondii*, DFT, Molecular docking.

Introduction

Visceral leishmaniasis (VL) is the most severe clinical form of leishmaniasis and is caused by protozoan parasites of the genus *Leishmania*, which are primarily transmitted through the bites of infected female phlebotomine sandflies [1][2][3]. VL remains an important neglected tropical disease, particularly affecting populations living in endemic regions where malnutrition, poverty, population displacement, inadequate housing, and immunosuppression increase the risk of infection and severe disease. If left untreated, VL can be fatal, especially in immunocompromised individuals. Despite the substantial progress made in understanding the disease, effective preventive measures remain limited, and pharmacological treatment continues to be the principal strategy for disease management [4][5]. The current therapeutic arsenal includes pentavalent antimonials, amphotericin B formulations, miltefosine, and paromomycin. However, the clinical use of several of these agents is limited by toxicity, adverse effects, high treatment costs, prolonged therapeutic regimens, and, in some endemic areas, the emergence of drug resistance [6][7]. These limitations highlight the need for the continuous development of new antileishmanial compounds with improved efficacy, safety, and pharmacological profiles. In this regard, rational drug design and the identification of structurally diverse bioactive scaffolds represent important approaches in the search for novel therapeutic candidates [8]. In this context, Heterocyclic compounds occupy a central position in medicinal chemistry because of their structural diversity, tunable physicochemical properties, and ability to interact with a wide range of biological targets [9][10][11]. Their importance in drug discovery is reflected by the presence of heterocyclic motifs in numerous biologically active and clinically relevant molecules [12]. Accordingly, considerable efforts have been devoted to the design and synthesis of heterocyclic derivatives with antiparasitic, antimicrobial, anticancer, anti-inflammatory, antidiabetic, and antiviral activities [13][14][15][16][17].. Among these scaffolds, thiazolidinones have attracted particular attention because of their versatile chemistry and broad pharmacological potential. The thiazolidinone nucleus is a well-established pharmacophore in medicinal chemistry and has been incorporated into compounds displaying diverse biological activities, including antiparasitic [16], anticancer [11][18][19][20][21][22], antimalarial [23], antidiabetic [24], anti-inflammatory [25], anti-HIV [26][27], anti-Alzheimer's [28], anti-infective [29], and antioxidant activities [18]. The pharmaceutical relevance of this scaffold is further illustrated by the thiazolidinedione/glitazone class, including pioglitazone, which has been widely used in the treatment of type 2 diabetes and related metabolic disorders [30][31][32]. Importantly, previous studies have also demonstrated the antiparasitic potential of thiosemicarbazone and thiazolidinone derivatives. For example, Oliveira Filho et al. reported thiazolidinone derivatives with significant anti-*Trypanosoma cruzi* activity, including promising in vivo effects in murine models [16]. Although *T. cruzi* is the causative parasite of Chagas disease rather than leishmaniasis, these findings support the broader antiparasitic potential of the thiazolidinone scaffold (Compounds I and II, Scheme 1). Based on these considerations, the development of new

thiazolidinone-based derivatives represents a promising strategy for the discovery of structurally novel antiparasitic agents. In the present study, we designed and synthesized a novel series of thiazolidinone derivatives derived from (R)-camphor-based thiosemicarbazone hybrids. The synthesized compounds were characterized using appropriate spectroscopic and analytical techniques and subsequently evaluated for their antileishmanial activity. Molecular docking and complementary computational studies were also performed to investigate their potential interactions with relevant biological targets and to provide structural insights into their observed activity. This integrated experimental and computational approach was undertaken to identify new thiazolidinone-based molecular frameworks with potential for further development as antileishmanial candidates.



Scheme 1: Molecular hybridization-based design of the novel thiazolidinones as potential anti-Trypanosomatidae agents.

Therefore, this study aimed to synthesize a novel series of thiosemicarbazone and thiazolidinone derivatives (Scheme 1) and to evaluate their biological potential through ADME profiling, molecular docking studies, and *in vitro* assays assessing cytotoxicity and antiparasitic activity against *Toxoplasma gondii* and both the promastigote and amastigote forms of *Leishmania major*.

Experimental

Materials and methods

All the chemicals and solvents required for the synthesis of compounds were purchased from Merck and Sigma-Aldrich. Thin-layer chromatography (TLC) was performed using F254 percolated plates (0.25 mm) and visualized by UV fluorescence. Column chromatography purifications were performed

on silica gel 60 (230-400 Mesh) using hexane/ethyl acetate mixtures as the eluent. ^{1}H and ^{13}C NMR spectra were recorded at 500 and 125 MHz, respectively, on a Bruker Avance III spectrometer equipped with a BBFO probe at room temperature, using $CDCl_3$ as the solvent. Chemical shifts (δ) are expressed in parts per million (ppm). They were recorded relative to the solvent $CDCl_3$ signal (7.26 ppm and 77.16 ppm). HRMS was obtained on a Q-TOF micro mass spectrometer. The intermediate compounds **2a, 3a, 2c, 3c, 8a, and 8b** have been prepared and identified according to the reported procedures [33][34].

Procedure for the preparation of (R)-camphor-thiazolidinone (4a-c).

A mixture of (R)-camphor-thiosemicarbazone derivatives (**2a**-**2c**) (1 mmol) and ethyl bromoacetate (1 mmol) was prepared in 20 mL of absolute ethanol, in the presence of 3 equivalents of sodium bromoacetate. The reaction mixture was refluxed for about 4 hours and monitored by CCM. The excess solvent in the reaction mixture was evaporated under reduced pressure. The resulting residue was then diluted with water and extracted using ethyl acetate (EtOAc) (3 × 25 mL). The combined organic layers were dried over anhydrous sodium sulfate (Na_2SO_4). After evaporation of the solvent, the crude product was purified by silica gel column chromatography to afford thiazolidinones **(4a-c)**.

(E)-N-methyl-2-((1S,4R)-1,7,7-trimethylbicyclo[2.2.1]heptan-2-ylidene)hydrazine-1-carbothioamide (2b)

Yield: 72%; m.p: 160-162 °C (Ethanol).^{1}H NMR (300 MHz, $CDCl_3$, TMS, δ in ppm) : 8.29 (1H monoxide , s, NH); 7.47 (1H, s, NH); 3.22 (H-2'); 2.43 (1H, dd, (J3=3Hz), H-3); 2.03 (1H, t, (J3 =15Hz), H-3); 1.92(1H, d, (J2=15Hz and J2=3Hz), H-4); 1.2-1.42 and 1.71-1,91(2H, m, H-5 and H-6); 1.10; 1.04 and 0.74 (9H, s, H-8, H-9 and H-10). ^{13}C NMR (75 MHz, $CDCl_3$, TMS, δ in ppm): 178.55 (C1'); 165.33 (C2); 52.70 (C7); 48.08 (C1); 43.97 (C4); 33.82 (C3); 31.02 (C2'); 32.55 and 27.16 (C5 and C6); 19.43; 18.58 and 11.13 (C8, C9 and C10). HRMS: m/z $[M + H]^+$ Calcd for $C_{12}H_{22}N_3S$: 240.1529; found: 240.1530.

(E)-N-phenyl-2-((1S,4R)-1,7,7-trimethylbicyclo[2.2.1]heptan-2-ylidene)hydrazine-1-carbothioamide (2c)

Yield: 62%; m.p.: 198-200 °C (Ethanol). ^{1}H NMR (300 MHz, $CDCl_3$, TMS, δ in ppm): 8.42 (1H, s, NH); 9.26 (1H, s, NH); 7.10-7.70 (5H, m, H-Ph); 2.45 (1H, dd, (J2=3.5Hz), H-3); 1.94(1H, d, (J2=15Hz and J3=18Hz), H-3); 2.05 (1H, m, H-4); 1.2-1.45 and 1.78-1.82 (4H, m, H-5 and H-6); 0.77 and 0.95 and 1.04 (9H, s, H-8, H-9 and H10). ^{13}C NMR (75 MHz, $CDCl_3$, TMS, δ in ppm): 176.04 (C1'); 165.98 (C2); 138.23 (C2'); 124.00-128.64 (C3'-C5'); 52.95 (C7); 44.11 (C4); 34.06 (C3); 32.60 and 27.19 (C5 and C6); 19.50; 18.60 and11.09 (C8, C9 and C10). HRMS: m/z (TOF-MS ES+) $(M+H^{1+})$ Calcd for $C_{17}H_{24}N_3S$: 302, 1685 found, 302.1685.

(E)-3-methyl-2-(((1S,4R,E)-1,7,7-trimethylbicyclo[2.2.1]heptan-2-ylidene)hydrazono)thiazolidin-4-one (4b)

Yield: 71%; m.p: 226-228 °C (Ethanol).^{1}H NMR (600.16MHz, $CDCl_3$, TMS, δ in ppm): 3.71 (2H, s, H-5'); 3.23 (3H, s, H6'); 2.64 (1H, dd, (J2=18.18Hz and J3=3.78Hz), H-3); 2.15 (1H, d,2(J=4.38Hz),

H-4); 1.22-1.88 (4H, m, H-5 and H-6); 1.91 (1H, t, (J3=17.12), H-3); 1.05, 0.94 and 0.79 (9H, s ,H-8, H-9 and H-10).^{13}C NMR (150.75 MHz, $CDCl_3$, TMS, δ in ppm): 181.01 (C2); 172.30 (C4'); 159.73 (C2'), 53.05 (C7); 48.13 (C1); 44.02 (C4); 36.11 (C3); 32.47 (C5'); 29.71 (C6'); 32.86 and 27.42 (C5 and C6); 19.77 (C10); 18.92 and 11.25 (C8 and C9). HRMS: m/z (TOF-MS ES+) ($M+Na^+$) Calcd for $C_{14}H_{21}N_3ONaS$: 302.1298 found, 302.1308.

(E)-3-phenyl-2-(((1S,4R,E)-1,7,7-trimethylbicyclo[2.2.1]heptan-2-ylidene)hydrazono)thiazolidin-4-one (4c)

Yield: 67%; m. p: 249-251 °C (Ethanol). ^{1}H NMR (300 MHz, $CDCl_3$, TMS, δ in ppm): 7.33-7.50 (5H, m, H-7', H-8' and H-9'); 3.85 (2H, s, H-5'); 2.36 (1H, dd, (J_2 =18Hz) and J_3=3Hz, H-3); 1.89 (1H, d, J_2=18 Hz, H-3); 1.82 (1H, t, (J_3 =6Hz), H-4); 1.12-1.81 (2H, m, H5 and H-6); 1.06, 0.92 and 0.76 (9H, s, H-8, H-9 and H-10). ^{13}C NMR (75 MHz, $CDCl_3$, TMS, δ in ppm): 181.06 (C2); 171.69 (C4'); 159.02 (C2'); 134.84 (C6'); 127.68-129.03 (C7'- C9'); 52.94 (C7); 48.05 (C1); 43.83 (C4); 36.02 (C3); 32.43 (C5'); 32.71 and 27.21 (C5 and C6); 19.69, 18.82 and 11.17 (C8, C9 and C10). HRMS: m/z (TOF-MS ES+) $(M+H)^+$ Calcd for $C_{19}H_{24}N_3OS$: 341.1635 found, 342.1635

Synthesis of compounds (6a-8c):

A solution of compounds (**4a-c)** (1.1 mmol) and benzaldehyde derivatives (1.3 mmol) in toluene (10 mL) was stirred at reflux for 6-8 hours. After the reaction was completed (monitored by TLC), the mixture was poured into water, extracted with ethyl acetate, and dried over anhydrous Sodium Sulfate. Evaporation of the solvent and recrystallization from a hexane-ethyl acetate mixture gave the desired product.

(E)-5-((E)-benzylidene)-3-methyl-2-(((1S,4R,E)-1,7,7-trimethylbicyclo[2.2.1]heptan-2-ylidene) hydrazono)thiazolidin-4-one (6a)

Yield: 71%; m. p: 200-202 °C (Ethanol). ^{1}H NMR (500.13 MHz, $CDCl_3$, TMS, δ in ppm): 7.69 (1H, s, H-6'); 7.58 (2H, d, (J2=7.6Hz), H-ph); 7.47 (2H, dd, (J2 =7.35), H-ph); 2.74 (1H, m, H-3); 2.24 (1H, d, (J_2=7.55Hz and J_2=7.75H), H-ph); 7.39 (1H, t, (J_2=17.85Hz), H3); 1.96 (1H, t, (J_3=4.20Hz), H-4); 1.47-1.83 and 1.27-1.91 (4H, m, H-6 and H-5); 1.13, 0.97 and 0.86 (9H, s ,H8, H-9 and H-10). ^{13}C NMR (125.75 MHz, $CDCl_3$, TMS, δ in ppm): 181.42 (C2); 168.18 (C4'); 157.71 (C2'); 134.05 (C7'); 130.84 (C6'); 130.24 (C8'); 129.80 (C10'); 129.14 (C9'); 122.94 (C5'); 53.50 (C7); 48.19 (C1); 44.14 (C4); 36.25 (C3); 32.98 and 27.32 (C5 and C6); 19.78, 18.92 and 11.40 (C8, C9 and C10). HRMS: m/z (TOF-MS ES+) ($M+H^+$) Calcd for $C_{20}H_{24}N_3OS$: 353.1635 found, 354.1635

(E)-5-((E)-4-chlorobenzylidene)-2-(((1S,4R,E)-1,7,7-trimethylbicyclo[2.2.1]heptan-2ylidene) hydrazono)thiazolidin-4-one (6b)

Yield: 84%; m.p: 234-236 °C (Ethanol).^{1}H NMR (500.13 MHz, $CDCl_3$, TMS, δ in ppm): 7.61 (1H, s, H-6'); 7.49 (2H, d, (J_2=8.5Hz), H-Ar); 7.44 (2H, d(J_3=8.5Hz), H-Ar); 2.73 (1H, m, H-3); 2.23 (1H, d, (J_2=17.9Hz), H-3); 1.95 (1H, t, (J_2=4.20 Hz), H-4); 1.47-1.79 and 1.29-1.87 (4H, m, H-6 and H-5);

1.12, 0.96 and 0.85 (9H,s , H8, H-9 and H-10). ^{13}C NMR (125.75 MHz, $CDCl_3$, TMS, δ in ppm): 181.68 (C2); 167.98 (C4'); 157.35 (C2'); 135.74 and 132.54 (C7' and C10'); 129.34 (C6'); 129.45 and 131.31 (C8' and C9'); 123.63 (C5'); 53.54 (C7); 48.20 (C1); 44.13 (C4); 36.29 (C3); 32.96 and 27.32 (C5 and C6); 19.78, 18.91 and 11.39 (C8, C9 and C10). HRMS: m/z (TOF-MS ES+) $(M+H)^+$ Calcd for $C_{20}H_{23}ClN_3OS$: 388.1245 found, 388.1245

(E)-5-((E)-4-nitrobenzylidene)-2-(((1S,4R,E)-1,7,7-trimethylbicyclo[2.2.1]heptan-2-ylidene) hydrazono)thiazolidin-4-one (6c)

Yield: 63%; m.p.: 246-248 °C (Ethanol). ^{1}H NMR (300 MHz, $CDCl_3$, TMS, δ in ppm): 7.68 (1H, s, H-6'); 8.33 (2H, d, (J_3=9Hz),H-Ar); 2.73 (1H, d large, (J3=9Hz), H-Ar); 7.70 (2H, d, (J_3=18Hz), H-3); 2.21 (1H, d, (J_2=18Hz), H-3); 1.96 (1H, m, H-4); 1.47-1.97 (4H, m, H-6 and H-5); 1.12, 0.97 and 0.84 (9H, s, H-8, H-9 and H-10). ^{13}C NMR (75 MHz, $CDCl_3$, TMS, δ in ppm): 182.41 (C2); 167.51 (C4'); 156.35 (C2'); 140.28 and 127.81 (C7' and C10'); 127.51 (C6'); 124.37 and 130,57 (C8' and C9'); 123.63 (C5'); 53.64 (C7); 48.26 (C1); 44.12 (C4); 36.38 (C3); 32.94 and 27.32 (C5 and C6); 19.76, 18.90 and 11.36 (C8, C9 and C10). HRMS: m/z (TOF-MS ES+) $(M+H^+)$ Calcd for $C_{20}H_{23}N_4O_3S$:399.1485 found, 399.1485

(E)-5-((E)-benzylidene)-3-methyl-2-(((1S,4R,E)-1,7,7-trimethylbicyclo[2.2.1]heptan-2-ylidene) hydrazono)thiazolidin-4-one (7a)

Yield: 74%; m.p.: 180-182 °C (Ethanol). ^{1}H NMR (300 MHz, $CDCl_3$, TMS, δ in ppm):7.67 (1H, s, H-7'); 7.58 (2H, d, (J_3=6Hz), H-Ar); 7.36-7.47 (3H, m, H-Ar); 3.38 (3H, s, H6'); 2.64 (1H, m, H-3); 2.16 (1H, d, (J_2=18Hz), H-3); 1.95 (1H, t, (J_3=6Hz), H-4); 1.75-1.82 and 1.22-1.51 (4H, m, H-6 and H-5); 1.13, 0.96 and 0.82 (9H, s, H-8, H-9 and H-10).^{13}C NMR (75 MHz, $CDCl_3$, TMS, δ in ppm): 181.61 (C2); 167.07 (C4'); 156.06 (C2'); 134.22 (C8'); 129.85 (C7'); 130.06 (C9'); 129.44 (C11'); 128.98 (C10'); 122.78 (C5'); 53.08 (C7); 48.09 (C1); 43.94 (C4); 36.24 (C3); 32.82 and 27.35 (C5 and C6); 29.70 (C6'); 19.70, 18.83 and11.28 (C8, C9 and C10). HRMS: m/z (TOF-MS ES+) $(M+H)^+$ Calcd for $C_{21}H_{26}N_3OS$: 368.1791 found, 368.1791.

(E)-5-((E)-4-chlorobenzylidene)-3-methyl-2-(((1S,4R,E)-1,7,7-trimethylbicyclo[2.2.1]heptan-2-ylidene) hydrazono)thiazolidin-4-one (7b)

Yield: 81%; m.p: 222-224 °C (Ethanol).^{1}H NMR (300 MHz, $CDCl_3$, TMS, δ in ppm):7.60 (1H, s, H-7'); 7.40-7.51 (4H, m, H-9'and H10'); 3.39 (3H, s, H-6'); 2.64 (1H, m, H-3); 2.17 (1H, d, (J_2=18Hz), H-3); 1.95 (1H, t, (J_3=6Hz), H-4); 1.72-1.83 and 1.19-1.51 (4H, m, H-6 and H-5); 1.12, 0.96 and 0.82 (9H, s, H-8, H-9 and H-10).^{13}C NMR (75 MHz, $CDCl_3$, TMS, δ in ppm): 182.07 (C2); 166.99 (C4'); 155.78 (C2'); 135.42 (C8'); 128.43 (C7'); 131.23 (C9'); 132.80 (C11'); 129.35 (C10'); 123.57 (C5'); 53.21 (C7); 48.20 (C1); 44.01 (C4); 36.35 (C3); 32.89 and 27.41 (C5 and C6); 29.86 (C6'); 19.77, 18.90 and 11.34 (C8, C9 and C10). HRMS: m/z (TOF-MS ES+) $(M+H)^+$ Calcd for $C_{21}H_{25}ClN_3OS$: 402.1401 found, 402.1401.

(E)-3-methyl-5-((E)-4-nitrobenzylidene)-2-(((1S,4R,E)-1,7,7-trimethylbicyclo[2.2.1]heptan-2-ylidene) hydrazono)thiazolidin-4-one (7c)

Yield: 60%. m.p: 260-262 °C (Ethanol). ^{1}H NMR (300 MHz, $CDCl_3$, TMS, δ in ppm): (J3 =9Hz), HAr); 7.63 (1H, s, H-7'); 7.66-7.69 (2H, m, H-Ar); 3.38 (3H, s, H-6'); 2.63 (1H, m, H-3); 2.16 (1H, d, 8.27 (2H, d, (J_2=18Hz), H-3) ; 1.94(1H, t, (J_3=6Hz), H-4) ; 1.74-1.81 and 1.21-1.49 (4H, m, H-6 and H-5); 1.10, 0.95 and 0.80 (9H,s , H-8, H-9 and H-10).^{13}C NMR (75 MHz, $CDCl_3$, TMS, δ in ppm):182.82 (C2); 166.42 (C4'); 155.02 (C2'); 147.36 (C8'); 126.56 (C7'); 130.44 (C9'); 132.80 (C11'); 124.23 (C10'); 127.66 (C5'); 53.28 (C7); 48.20 (C1); 43.94 (C4); 36.39 (C3); 32.82 and 27.34 (C5 and C6); 30.01(C6'); 19.71, 18.84 and 11.28 (C8, C9 and C10).HRMS: m/z (TOF-MS ES+) $(M+H)^+$ Calcd for $C_{21}H_{25}N_4O_3S$: 413.1642 found, 413.1642.

(E)-5-((E)-benzylidene)-3-phenyl-2-(((1S,4R,E)-1,7,7-trimethylbicyclo[2.2.1]heptan-2ylidene)hydrazono) thiazolidin-4-one (8a)

Yield: 68%, m.p: 231-233 °C (Ethanol).^{1}H NMR (300 MHz, $CDCl_3$, TMS, δ in ppm):7.79 (1H, s, H-10'); 7.40-7.65 (10H, m, H-7', H-8', H-9' and H-12', H-13' and H-14'); 2.45 (1H, m, H-3); 1.98 (1H, d, (J_2 =18Hz), H-3); 1.88 (1H, t,: (J_3=6Hz), H-4); 1.75-1.81 and 1.18-1.60 (4H, m, H-6 and H-5); 1.15, 0.95 and 0.80 (9H, s, H-8, H-9 and H-10).^{13}C NMR (75 MHz, $CDCl_3$, TMS, δ in ppm): 182.21 (C2); 166.71 (C4'); 155.54 (C2'); 128.59 (C10'); 130.61 and 129.66 (C9' and C14'); 127.80 and 129.04 and 129.14 and 130.26 (C7' and C12'); 134.32 and 134.98 (C6' and C11'); 122.48 (C5'); 53.20 (C7); 48.22 (C1); 43.94 (C4); 36.36 (C3); 32.85 and 27.29 (C5 and C6); 19.78, 18.88 and 11.33 (C8, C9 and C10).HRMS: m/z (TOF-MS ES+) $(M+H)^+$ Calcd for $C_{26}H_{28}N_3OS$: 430.1948 found, 430.1948.

(E)-5-((E)-4-chlorobenzylidene)-3-phenyl-2-(((1S,4R,E)-1,7,7-trimethylbicyclo[2.2.1]heptan-2-ylidene) hydrazono)thiazolidin-4-one (8b)

Yield: 77%; m.p: 272-274 °C (Ethanol).^{1}H NMR (300 MHz, $CDCl_3$, TMS, δ in ppm):7.69 (1H, s, H-10'); 7.41-7.56 (9H, m, H-7', H-8', H-9', H-12' and H-13'); 2.42 (1H, m, H-3); 1.94 (1H, d, (J2=18 Hz), H-3); 1.86 (1H, t, (J3=6 Hz), H-4); 1.60-1.79 and 1.16-1.50 (4H, m, H-6 and H-5); 1.11, 0.93 and 0.77 (9H, s, H-8, H-8 and H-10).^{13}C NMR (75 MHz, $CDCl_3$, TMS, δ in ppm): 182.38 (C2); 166.49 (C4'); 155.21 (C2'); 128.63 (C10'); 132.97 (C14'); 127.81 and 129.05 and 129.46 and 131.34 (C7' - C18' and C12'-C13'); 135.62 and 135.05 (C6' and C11'); 123.44 (C5'); 53.28 (C7); 48.26 (C1); 44.07 (C4); 36.42 (C3); 32.94 and 27.34 (C5 and C6); 19.79, 18.90 and 11.30 (C8, C9 and C10). HRMS: m/z (TOF-MS ES+) $(M+H)^+$ Calcd for $C_{26}H_{27}ClN_3OS$: 464,1558 found, 464.1558.

(E)-5-((E)-4-nitrobenzylidene)-3-phenyl-2-(((1S,4R,E)-1,7,7-trimethylbicyclo[2.2.1]heptan-2-ylidene)hydrazono)thiazolidin-4-one (8c)

Yield: 55%; m.p: 235-237 °C (Ethanol).^{1}H NMR (300 MHz, $CDCl_3$, TMS, δ in ppm): 7.75 (1H, s, H-10'); 8.34 (2H, d, (J3=9Hz), H-Ar); 7.76 (2H, m, H-Ar); 7.42-7.51 (2H, m, H-Ar); 2.44 (1H, m, H-3); 1.96 (1H, d, (J2=18Hz), H-3); 1.85 (1H, t, (J2=6 Hz), H-4); 1.75-1.80 and 1.17-1.50 (4H, m, H-6 and

H-5); 1.12, 0.94 and 0.78 (9H, s ,H-8, H-9 and H-10).^{13}C NMR (75 MHz, $CDCl_3$, TMS, δ in ppm): 183.21 (C2); 166.03 (C4'); 154.61 (C2'); 127.24 (C10'); 134.83 (C14'); 130.59 and 129.15 and 128.85 and 127.71 and 124.38 (C7'-C9' and C12'-C13'); 147.68 and 140.68 (C6' and C11'); 127.58 (C5'); 53.41 (C7); 48.32 (C1); 44.07 (C4); 36.52 (C3); 32.94 and 27.33 (C5 and C6); 19.79, 18.89 and 11.30 (C8, C9 and C10).HRMS: m/z (TOF-MS ES+) $(M+H)^+$ Calcd for $C_{26}H_{27}N_4O_3S$: 475.1798 found, 475.1798.

Synthesis of compounds 5a-c :

Compounds (**4a-c)** (1 mmol) reacted with *N*, *N*-Dimethylformamide dimethyl acetal (DMF-DMA) (1 mmol) in DMF (8 mL) under reflux conditions for 6-8 hours, after completion of the reaction (monitored by TLC). After the reaction was complete (as confirmed by TLC), the mixture was poured into cold water, and the precipitate was filtered and washed with petroleum ether to afford compounds (**5a-c**).

(2E,5Z)-5-((dimethylamino)methylene)-2-((E)-(1,7,7-trimethylbicyclo[2.2.1]heptan-2-ylidene) hydrazono)thiazolidin-4-one (5a)

Yield: 34%; m.p: 250-252 °C (Ethanol).^{1}H NMR (600.16 MHz, $CDCl_3$, TMS, δ in ppm): 7.37 (1H, s, H-6'); 3.12 (6H, s, (H-7' and H-8'); 2.62 (1H, dd, (J2=17.82 and J3=3.90 Hz, H-3) and 2.13 (1H,d, (J2=17.88 Hz), H-3); 1.90 (1H, t, (J3=4.32Hz), H-4); 1.23 – 1.86 (4H,m, H-5 and H-6); 1.05, 0.93 and 0.80 (9H,s, (H-8, H-9 and H-10).^{13}C NMR (150.75 MHz, $CDCl_3$, TMS, δ in ppm): 178.10 (C2); 169.50 (C4'); 158.91 (C2'); 143.45 (C6'); 88.17 (C5'); 53.01 (C7); 48.06 (C1); 44.18 (C4); 42.34 (C7' and C8'); 36.08 (C3); 33.04 and 27.43 (C5 and C6); 19.81, 18.95 and 11.43 (C8, C9 and C10).HRMS: m/z (TOF-MS ES+) $(M+H)^+$ Calcd for $C_{16}H_{25}N_4OS$: 321.1744 found, 321.1727.

(2E,5Z)-5-((dimethylamino)methylene)-3-methyl-2-((E)-(1,7,7-trimethylbicyclo[2.2.1]heptan-2-ylidene)hydrazono)thiazolidinone (5b).

Yield: 8%; m.p: 230-232 °C (Ethanol). ^{1}H NMR (600.16 MHz, $CDCl_3$, TMS, δ in ppm): 7.39 (1H, s, H-6'); 3.26 (3H, s, H-9'); 3.12 (6H, s, (H-7' and H-8'); 2.59 (1H, dd, (J2=18.06 Hz and J3=3.90 Hz), H-3) and 2.14 (1H, d, (J3=18.12 Hz), H-3); 1.91 (1H, t, (J3=4.38 Hz), H-4); 1.23-1.88 (4H, m, H-5 and H-6); 1.08, 0.94 and 0.80 (9H, s, (H-8, H-9 and H-10).^{13}C NMR (150.75 MHz, $CDCl_3$, TMS, δ in ppm): 178.77 (C2); 168.86 (C4'); 158.51 (C2'); 142.95 (C6'); 88.16 (C5'); 52.87 (C7); 48.12 (C1); 44.12 (C4); 42.36 (C7' and C8'); 36.12 (C3); 29.28 (C9'); 33.02 and 27.49 (C5 and C6); 19.81, 18.85 and 11.42 (C8, C9 and C10).HRMS: m/z (TOF-MS ES+) $(M+H)^+$ Calcd for $C_{17}H_{27}N_4OS$: 335.1900 found, 335.1910.

(2E,5E)-5-((dimethylamino)methylene)-3-phenyl-2-(((1S,4R,E)-1,7,7-trimethylbicyclo[2.2.1]heptan-2-ylidene)hydrazono)thiazolidin-4-one (5c)

Yield: 70%; m.p: 238-240 °C (Ethanol).^{1}H NMR (300 MHz, $CDCl_3$, TMS, δ in ppm):7.43 (1H, s, H-6'); 7.29-7.44 (5H, m, H-10', H-11' and H-12'); 3.07 (6H, s, (H-7' and H-8'); 2.38 (1H, dd, (J2 =18.00

Hz), H3); 1.79 (1H, t, (J2=18.00 and J3=3.00 Hz), H-3) and 1.91 (1H, d, (J2=3Hz), H-4); 1.10-1.73 (4H, m, H-5 and H-6); 1.06, 0.89 and 0.74 (9H, s, (H-8, H-9 and H-10).^{13}C NMR (75 MHz, $CDCl_3$, TMS, δ in ppm): 178.74 (C2); 167.82 (C4'); 157.26(C2'); 143.23 (C6'); 135.57 (C9'); 128.43, 127.74 and 127.53 (C10', C11' and C12'); 87.16 (C5'); 52.49 (C7); 43.68 (C4); 47.78 (C1); 42.06 (C7' and C8'); 35.84 (C3); 32.64 and 27.05 (C5 and C6); 19.52, 18.63 and11.11 (C8, C9 and C10). HRMS: m/z (TOF-MS ES+) $(M+H)^+$ Calcd for $C_{22}H_{29}N_4OS$: 397.2057 found, 397.2057.

Synthesis of compounds (3a-c):

A mixture of (R)-camphor-thiosemicarbazone derivatives (**2a**, **2c**) and dimethyl acetylenedicarboxylate (1.25 eq) in anhydrous MeCN (20 mL) was stirred under reflux for 30 min. After the reaction was completed (TLC monitored its progress), the solvent was evaporated to dryness. The crude product was purified by silica gel chromatography (230–400 mesh) using hexane/ethyl acetate as an eluent. The pure thiazole products **(3a-c)** were obtained in good yields.

Methyl(E)-2-((E)-4-oxo-2-(((1S,4R,E)-1,7,7-trimethylbicyclo[2.2.1]heptan-2-ylidene)hydrazono) thiazolidin-5-ylidene)acetate (3a)

Yield: 79%; m.p: 230-232 °C (Ethanol).^{1}H NMR (500.13 MHz, $CDCl_3$, TMS, δ in ppm):10.71 (1H, s, NH); 6.84 (1H, s, H-6'); 3.12 (6H 3.84 (3H, s, H-8'); 2.66 (1H, dd, (J2=17.75Hz and J2 3=17.9Hz), H-3); 1.93 (1H, t, (J3=3.15Hz), H-3); 2.17 (1H, d, (J2=4.15Hz), H-4); 1.22 -1.48 and 1.73 -1.88 (4H, m, H-5 andH-6); 1.07, 0.94 and 0.81 (9H, s, H-8, H-9 and H-10).^{13}C NMR (125.75 MHz, $CDCl_3$, TMS, δ in ppm): 182.52 (C2); 166.56 (C7'); 166.13 (C4'); 158.42 (C2'); 142.73 (C5'); 116.09 (C6'); 53.28 (C7); 52.61 (C8'); 48.17 (C1); 44.09 (C4); 36.13 (C3); 32.83 and 27,25 (C5 and C6); 19.72, 18.87 and 11.22 (C8, C9 and C10). HRMS: m/z (TOF-MS ES+) $(M+H)^+$ Calcd for $C_{16}H_{21}N_3O_3S$: 336.1376 found, 335.4220.

methyl(E)-2-((E)-3-methyl-4-oxo-2-(((1S,4R,E)-1,7,7-trimethylbicyclo[2.2.1]heptan-2-ylidene) hydrazono)thiazolidin-5-ylidene)acetate (3b)

Yield: 72%; m.p: 204-206 °C (Ethanol).^{1}H NMR (300 MHz, $CDCl_3$, TMS, δ in ppm): 6.84 (1H, s, H-6'); 3.84 (3H, s, H-8'); 3.36 (3H, s, H-9'); 2.60 (1H, dd, (J3=3.15Hz), H-3); 2.12 (1H, m, H-3); 1.93 (1H, t, (J3=18Hz and J3=6Hz), H-4); 1.45 and 1.76 (2H, m, H-5); 1.26 and 1.85 (2H, m, H-6); 1.06, 0.94 and 0.79 (6H, s, H-8, H-9 and H-10). ^{13}C NMR (75 MHz, $CDCl_3$, TMS, δ in ppm): 182.89 (C2); 166.66 (C7'); 165.29 (C4'); 156.42 (C2'); 142.70 (C5'); 115.26 (C6'); 53.35 (C7); 52.48 (C8'); 48.19 (C1); 43.99 (C4); 36.23 (C3); 29.63 (C9'); 32.78 and 27.38 (C5 and C6); 19.74, 18.88 and 11.20 (C8, C9 and C10). HRMS: m/z (TOF-MS ES+) $(M+H)^+$ Calcd for $C_{17}H_{24}N_3O_3S$: 350.1533 found, 349.1460.

methyl(E)-2-((E)-4-oxo-3-phenyl-2-(((1S,4R,E)-1,7,7-trimethylbicyclo[2.2.1]heptan-2ylidene) hydrazono)thiazolidin-5-ylidene)acetate (3c)

Yield: 65%; m.p: 242-244 °C (Ethanol).^{1}H NMR (300 MHz, $CDCl_3$, TMS, δ in ppm): 6.93 (1H, s, H-6'); 7.38-7.48 (5H, m, H-10', H-11' and H-12'); 3.86 (3H, s, H-8'); 2.40 (1H, m, H-3); 1.90 (1H, d,

(J2=18Hz), H-3); 1.78 (1H, t, (J3=6Hz), H-4); 1.17 – 1.74 (4H, m, H-5 and H-6); 1.08, 0.75 and 0.92 (9H, s ,H-8, H-9 and H-10).^{13}C NMR (75 MHz, $CDCl_3$, TMS, δ in ppm): 183.04 (C2); 166.64 (C7'); 164.73 (C4'); 155.98 (C2'); 142.45 (C5'); 115.73 (C6'); 127.61-129.05 (CPh); 53.37 (C7); 52.43 (C8'); 48.21 (C1); 44.03 (C4); 36.27 (C3); 32.81 and 27.28 (C5 and C6); 19.74, 18.84 and 11,14 (C8, C9 and C10). HRMS: m/z (TOF-MS ES+) $(M+H)^+$ Calcd for $C_{22}H_{26}N_3O_3S$: 412.1689 found, 411.5200.

Antiparasitic activity of selected compounds

***Toxoplasma gondii* bioactivity assay.**

In this technique, our previously published method was followed [35]. Tachyzoites RH strain of the *T. gondii* were cultivated in vero cells, then complete RPMI 1640 medium (Invitrogen, USA) with 10% fetal bovine serum (FBS, Invitrogen, USA) was used for culturing vero cells in 96-well plates (5×10^3 cells/well in 200 µL of medium), then incubated at 37 °C and under 5% CO_2 for 24 hours, after that *T. gondii* tachyzoites (RH strain) at a ratio of 5 (parasite): 1 (Vero cells) was inoculated to the cells. Then, after incubation at 37 °C under 5% CO2 for 5 hours, the cells were washed with PBS and overlaid with medium containing one of the tested compounds or atovaquone (ATO) at 20, 10, 5, 2.5, 1.25, 0.63, 0.32, … µg/mL. After 3 days of incubation, cells were stained with 1% toluidine blue and examined under an inverted photomicroscope (MCD-400, Leica, Japan) to determine the T. gondii infection index (number of infected cells among 200 tested cells). The experiment was performed in triplicate.

***Leishmania major* bioactivity assays**

We performed this method according to our previously published technique [35]. A group of mice of different sex was injected at the hind footpads with 1×10^6 *L. major* metacyclic promastigotes. *L. major* amastigotes were collected from the infected mice. Eight weeks after inoculation, Schneider's medium (Invitrogen, USA) containing antibiotics and 10% FBS was used to transform isolated amastigotes into promastigotes by incubation at 26 °C. Amastigote-derived promastigotes with less than five *in vitro* passages were used only for infections.

For the evaluation of the activity of the compounds against *L. major* promastigotes, 10^6 promastigotes/mL were cultured in 96-well plates in Schneider's medium with 10% FBS. Then, the compounds and amphotericin B (AmB) were added to obtain the final concentrations (20, 10, 5, 2.5, 1.25, 0.63, 0.32, … µg/mL). Negative control wells contained cultures with DMSO (1%) only. Plates were incubated at 26 °C for 72 h to evaluate the antiproliferative effect. The colorimetric MTT method was used to count viable promastigotes using a microplate absorbance spectrophotometer (xMark, Bio-Rad, USA) at an absorbance of 570 nm. The experiment was performed in triplicate.

Macrophage cells were obtained from the peritoneal activity of mice of different ages and sex and then used for culturing L. *major* amastigotes. To assess the activity of the compounds against amastigotes, we followed our previously published data [35]. Briefly, 1 mL of 3% Brewer's thioglycollate medium/mouse was injected into the peritoneal cavity. After four days, the abdominal

skin was removed to expose the peritoneal wall. Then, 3 mL of RPMI 1640 medium was injected before cells were collected by aspiration, whereupon 96-well plates containing RPMI 1640 medium with 10% FBS were used to culture 5×10^4 cells/well, which were incubated at 37 °C under 5% CO_2 for 4 h. After washing with PBS, RPMI 1640 medium containing 5×10^5 promastigotes was added to each well. Next, the cells were incubated at 37 °C under humidified 5% CO_2 for 24 hours to enhance infection and differentiation of amastigotes. Washing with PBS several times removes free promastigotes. Fresh complete RPMI 1640 medium containing one of the tested compounds or AmB at the desired final concentration (20, 10, 5, 2.5, 1.25, 0.63, 0.32, … µg/mL) was added and incubated at 37 °C under a humidified 5% CO_2 atmosphere for 72 h. DMSO (1%), only in complete RPMI medium, was used as the negative control. The percentage of infected macrophages was assessed microscopically after the medium was removed, followed by washing with PBS, fixation with methanol, and staining with Giemsa. The reading was performed in triplicate. The laboratory animals were handled according to the guidelines and regulations of the Committee of Research Ethics, Deanship of Scientific Research, Qassim University, as indicated by permission number 20-03-20.

Vero cell and macrophage cytotoxicity.

The MTT colorimetric assay was conducted to assess the cytotoxicity of the compounds, as previously published in our data [35]. Vero cells or macrophages were cultured in 96-well plates (5×10^3 cells/well/200 µL) in RPMI 1640 medium with 10% FBS at 37 °C and under 5% CO_2 overnight. Then PBS was used to wash the cells. Then, the compounds in RPMI complete medium with 10% FBS (at varying concentrations of 20, 10, 5, 2.5, 1.25, 0.63, 0.32, … µg/mL) were added to 96-well plates and incubated for 3 days. Cells treated with a medium containing only DMSO (1%) were used as the negative control. After washing, MTT (1 mg mL^{-1} in RPMI 1640 medium) was added to each well. The cells were incubated for 4 hours, and the supernatant was removed. Next, 150 µL of DMSO was added, and a microplate absorbance spectrophotometer was used for colorimetric analysis (λ = 540 nm). Cytotoxic effects were expressed by IC_{50} values (concentration that caused a 50% reduction of viable cells). The experiment was performed in triplicate.

Physicochemical and Pharmacokinetic Characteristics

The physicochemical and pharmacokinetic properties of the synthesized derivatives were evaluated using the SwissADME tool (http://www.swissadme.ch/). This in silico platform enabled a detailed analysis of key pharmacokinetic parameters, including absorption, distribution, metabolism, and excretion (ADME) [36]. The bioavailability radar chart within SwissADME employs sophisticated machine learning algorithms and statistical models, trained on extensive molecular datasets with well-defined pharmacological characteristics [37]. Furthermore, the BOILED-Egg model was utilized to predict critical ADME features such as blood-brain barrier (BBB) permeability, passive human

intestinal absorption (HIA), and classification of compounds as either substrates or non-substrates of the permeability glycoprotein (P-gp) [38].

Molecular Docking Analysis

Molecular docking was conducted to assess interactions between derivatives and target proteins with PDB ID 2jk6 (Trypanothione Reductase) and 2wuu (N-Myristoyltransferase). Protein models were prepared using MGL Tools by removing heteroatoms and water, adding polar hydrogens, and Kollman charges. After that, the protein structure was rendered and corrected for missing residues [39]. Synthesized derivatives were modeled and energy-minimized in ChemDraw 3D. We set grid box coordinates for the active sites: Trypanothione Reductase (x = 14.820410, y = 36.928390, z = 0.048730) and N-Myristoyltransferase (x = -8.322740, y = -24.088832, z = 18.189475). To validate the docking protocol, we removed the co-crystallized ligand from the Leishmania NMT PDB structure (2wuu) and redocked it into the active site using AutoDock Vina. The resulting poses were superimposed onto the original ligand, and the protocol was deemed successful upon achieving a Root Mean Square Deviation (RMSD) value of less than 2.0 Å. Analysis using docking was conducted on the target protein utilizing AutoDock Vina, with the default genetic algorithm serving as the scoring function. Docking was performed using AutoDock Vina with the num_modes parameter set to 100. The most stable pose (lowest binding energy) was analyzed in 2D and 3D for protein-ligand interactions [40][41].

Density Functional Theory

Density Functional Theory (DFT) analysis was carried out using the B3LYP/6-311++G(d,p) method to determine the electronic properties of the synthesized compounds. Geometry optimization, frequency calculations, Frontier Molecular Orbital (FMO) analysis, and global reactivity descriptors were computed using Gaussian 9w with the B3LYP/6-311++G(d,p) basis set [40]. GaussView 6 was used to visualize the output files [42]. The main aim is to determine the ground-state energy, charge distribution, and electronic behavior of a system, which helps explain how atoms bond or how chemical reactions occur. Furthermore, from DFT, we learn about structural stability, electronic and magnetic properties, and reaction energetics, allowing us to explain phenomena such as bonding, catalysis, magnetism, and conductivity on a microscopic level [43].

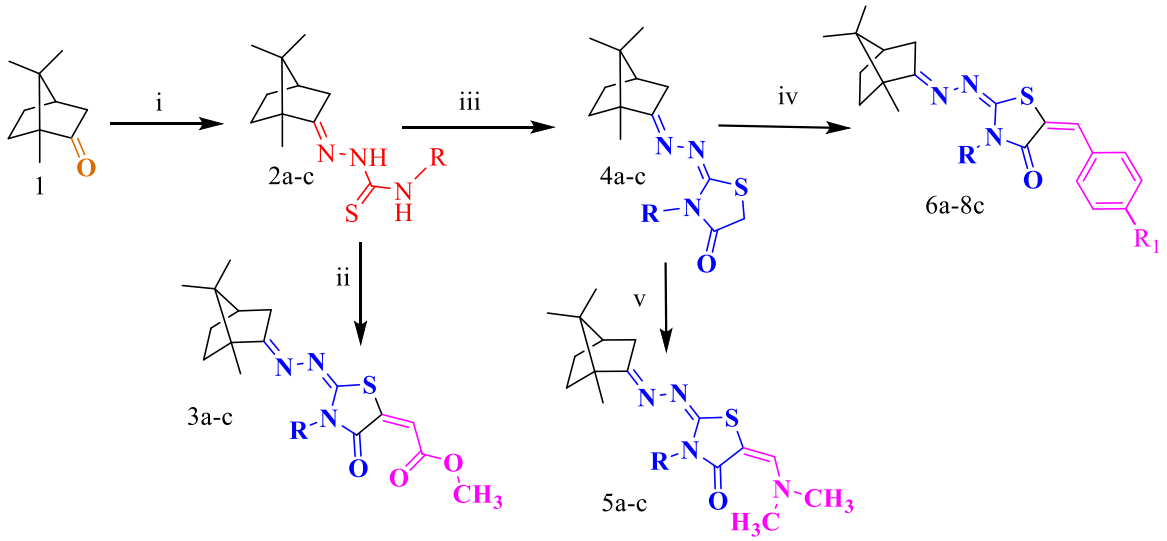
Results and Discussion

Synthesis and Characterization

The starting materials (compounds **2a**, **4a**, **2b**, **4b**, **5c**, and **5a**) and intermediates were synthesized according to methods previously reported by our group [33][34][44][45]. The synthetic pathway for preparing both intermediates and target compounds is illustrated in Scheme 2. Owing to its multiple reactive sites, the thiazolidinone ring can undergo diverse chemical transformations, including oxidation at the sulfur atom, N-alkylation, Mannich-type reactions, and condensations involving its

activated methylene groups. Cyclic sulfones derived from thiazolidinones are of significant interest in synthetic organic chemistry. The thiazolidinone scaffold contains two activated methylene groups: one adjacent to the carbonyl (C=O) group within the heterocyclic ring and the other at the α-position relative to the hydrazone moiety. Owing to this structural feature, compounds (**4a-c)** readily underwent condensation with *N, N*-dimethylformamide dimethyl acetal (DMF–DMA) under reflux conditions for 6–8 hours, affording compounds **(5a-c)**, respectively. The reactions proceeded smoothly, and the products were obtained in high yields after purification by silica gel column chromatography using a hexane/ethyl acetate gradient as the eluent.

Similarly, compounds **(4a-c)** were condensed with a series of benzaldehyde derivatives, providing the corresponding arylidene-substituted thiazolidinones (**6a-8c**) in satisfactory yields after chromatographic purification. Furthermore, thiosemicarbazone derivatives **2a-c** reacted efficiently with dimethyl acetylenedicarboxylate (DMAD) to furnish the ene-substituted thiazolidinone derivatives (**3a-c**).



Scheme 2: Synthetic routes to thiazolidinone derivatives.

Reagents and conditions: (i) thiosemicarbazides, EtOH, H_2SO_4 or HCl, rt, 1–2 hours; (ii) DMAD, MeCN, reflux, 30 min; (iii) ethyl 2-bromoacetate, NaOAc, EtOH, reflux, overnight; (iv) benzaldehyde derivatives, KOH, toluene, reflux, 1 hour; (v) DMF–DMA, KOH, toluene, reflux.

Table 1: Compounds 2a–c and 3a–8c were synthesized as thiosemicarbazone and thiazolidinone derivatives, respectively

Compounds	**R**	**Compounds**	R	**R1**
2a	H	6a	**H**	H
2b	CH_3	6b		Cl
2c	C_6H_5	6c		NO_2
3a	H	7a	**CH_3**	H
3b	CH_3l	7b		Cl
3c	C_6H_5	7c		NO_2
4a	H	8a		H

4b	CH_3	8b	**C_6H_5**	Cl
4c	C_6H_5	8c		NO_2
5a	H	-		
5b	CH_3	-		
5c	C_6H_5			

We confirmed the structures of all synthesized compounds by ^1H and ^{13}C NMR spectroscopy and high-resolution mass spectrometry (HRMS). For derivatives (**4a-c**), the formation of the heterocyclic system was confirmed by NMR spectroscopy. For example, the ^1H NMR spectrum of compound **4b** showed two singlets at 3.23 and 3.71 ppm, corresponding to the N–CH_3 protons and the ring methylene protons, respectively. Moreover, the ^{13}C NMR spectrum showed characteristic signals at 181.01 and 32.47 ppm, assigned to the carbonyl carbon and the methylene carbon, respectively. These spectral features clearly support the successful formation of the thiazolidinone scaffold.

On the other hand, the structures of the thiazolidinone-5-arylidene derivatives (**6a-8c**) were successfully confirmed by the same spectroscopic analyses. For example, the ^1H NMR spectrum of compound **6a** showed the disappearance of the methylene proton signal at around 3.7 ppm and the appearance of a singlet at 7.61 ppm, attributed to the ethylenic proton. In addition, the aromatic protons appeared as two doublets centered at 7.49 and 7.44 ppm. These spectral features confirm the successful condensation at the methylene position of the thiazolidinone core. As for the thiazolidinone derivatives **(5a-c)** and **(3a-c)**, comparable NMR features were observed. For instance, the ^1H NMR spectra of compounds **5a** and **3a** displayed the ethylenic proton at 7.37 and 6.84 ppm, respectively. In addition, compound **3a** was characterized by the presence of an N-$(CH_3)_2$ group, which appeared as a singlet integrating for six protons at 3.12 ppm, whereas compound **3a** showed a methoxy (O–CH_3) group resonating as a singlet integrating for three protons at 3.84 ppm. These signals are consistent with the proposed structures of these derivatives.

Biological activity

In vitro antileishmanial and antitoxoplasmal activity of the titled compounds

Table 2 indicates the activity of selected compounds against *L. major* promastigotes and amastigotes and *T. gondii in vitro* as well as their cytotoxic activity against host cells (macrophages and the Vero kidney cell line). Compound **2a** was found active against *L. major promastigotes*, amastigotes, and *T. gondii* with EC_{50} values of 0.5, 11.9, and 12.3 µg/mL, respectively, and SI values of 24.2, 1.1, and 0.42, respectively. Compounds **6a, 6b, 5c,** and **(3a-c)** were also found to be very active against *L. major* promastigotes with EC_{50} values of 6.1, 8.9, 3.8, 4.5, 8.6, and 7.8 µg/mL, respectively, and SI values of 3, > 2.3, 3.5, 2.9, 1.9, and 2.3, respectively. Compounds **(8a-c), 5a,** and **5c** revealed antitoxoplasmal activity against *T. gondii* with EC_{50} values less than 10 µg/mL and SI values of 1.9, 1.7, 2.2, 1.9, 1.2, and 1.0, respectively.

*Table 2. Effective concentrations (EC_{50}, in µg/mL) of compounds **(2a-8c)** against Leishmania major promastigotes (**prom**) and amastigotes (**ama**) and Toxoplasma gondii; IC_{50} (in µg/mL) of compounds **(2a-8c)** against macrophages (**macro**) and Vero (African green monkey kidney epithelial) cells. Amphotericin B (AmB) and atovaquone (ATO) were applied as positive controls.*

	EC_{50}			IC_{50}		SI		
	L. major		*T. gondii*	Vero	macro	*L. major*		Vero / *T. gondii*
	prom	ama				macro / prom	macro / ama	
2a	0.5	11.9	12.3	5.2	12.1	24.2	1.1	0.4
4a	> 20	10.2	> 20	4.9	13.9	-	1.4	-
2b	> 20	15.3	18.4	7.4	13.7	-	0.9	0.4
2c	> 20	> 20	> 20	> 20	> 20	-	-	-
4b	> 20	> 20	> 20	> 20	> 20	-	-	-
4c	> 20	> 20	> 20	> 20	> 20	-	-	-
6a	6.1	> 20	14.9	19.6	18.3	3	-	1.3
6b	8.9	> 20	> 20	> 20	> 20	>2.3	-	-
6c	> 20	> 20	> 20	> 20	> 20	-	-	-
7a	> 20	> 20	> 20	> 20	> 20	-	-	-
7b	> 20	> 20	> 20	> 20	> 20	-	-	-
7c	> 20	> 20	> 20	18.2	> 20	-	-	-
8a	> 20	> 20	9.5	18.4	18.4	-	-	1.9
8b	> 20	> 20	8.4	14.3	16.7	-	-	1.7
8c	12.4	> 20	8.7	19.1	18.1	1.5	-	2.2
5b	15.3	> 20	10.9	14.3	16.7	1.1	-	1.3
5a	14.7	> 20	9.2	15.2	19.2	1.3	-	1.7
5c	3.8	> 20	7.8	14.9	13.2	3.5	-	1.9
3a	4.5	> 20	13.1	15.5	13.2	2.9	-	1.2
3b	8.6	> 20	12.6	16.3	16.1	1.9	-	1.3
3c	7.8	> 20	18.8	18.4	17.9	2.3	-	1.0
AmB	0.83	0.47	—	10.3	8.1	12.4	17.2	-
ATO	—	—	0.21	28.5	-	—	—	135

n.d.: The selectivity index (SI) (IC_{50}/EC_{50}) was calculated from the corresponding IC_{50} against macrophages or Vero cells and EC_{50} against *L. major* promastigotes, amastigotes, and *T. gondii*.

Physicochemical and pharmacokinetic characteristics

All three compounds (**2a, 3a,** and **3b**) showed broadly similar predicted physicochemical and ADME profiles, with no major liabilities predicted by the applied in silico models. All compounds comply with Lipinski's rule of five with zero violations and show no PAINS or Brenk alerts, no predicted CYP inhibition, and no P-gp substrate liability, indicating a generally clean drug-likeness and safety profile. The predicted bioavailability scores were identical (0.55), while the synthetic accessibility scores were moderate, indicating comparable synthetic feasibility and potential for early-stage development, as shown in Table 2. Despite these similarities, the molecules differ mainly in size and polarity. Molecule **2a** is the smallest (MW 224.26) but also the most polar, with a high topological polar surface area (TPSA 147.33 Å²) and three hydrogen-bond donors, which strongly limit membrane permeability. Molecules **3a** and **3b** are larger (MW 335–349) but less polar, with lower TPSA values (105.42 and 96.63 Å², respectively), fewer or no hydrogen-bond donors, and higher fractions of sp^3 carbons, features that are generally more favorable for developability.

All three compounds are predicted to be highly soluble across multiple solubility models (ESOL, Ali, and Silicos-IT), consistent with their low consensus logP values (approximately −1.27). However, this high polarity and low lipophilicity also result in uniformly poor permeability, reflected in low predicted gastrointestinal absorption, lack of blood–brain barrier penetration, and very low skin permeability. Consequently, while none of the molecules present obvious toxicity or metabolic concerns, oral absorption is expected to be limited without further optimization Table 3.

Overall, Molecules **3a** and **3b** exhibit a more balanced physicochemical profile than Molecule 1, with Molecule **3a** being the least polar and most structurally complex, making it the most promising starting point for lead optimization if improved permeability and oral exposure are desired Table 3.

Table 3*:* Physicochemical and pharmacokinetic properties

Molecule	**2a**	**3a**	**3b**
Formula	$C_{11}H_{19}N_3S$	$C_{16}H_{21}N_3O_3S$	$C_{17}H_{23}N_3O_3S$
MW	225.35	335.42	349.45
#Heavy atoms	13	23	24
#Aromatic heavy atoms	0	0	0
Fraction Csp3	0.5	0.62	0.65
#Rotatable bonds	3	3	3
#H-bond acceptors	5	5	5
#H-bond donors	3	1	0
MR	55.22	94.85	99.75
TPSA	147.33	105.42	96.63
iLOGP	-0.3	-0.3	-0.3
XLOGP3	-0.6	-0.6	-0.6
WLOGP	-1.38	2.08	2.43
MLOGP	-2.75	-2.75	-2.75
Silicos-IT Log P	-1.3	-1.3	-1.3
Consensus Log P	-1.27	-1.27	-1.27
ESOL Log S	-0.65	-0.65	-0.65
ESOL Solubility (mg/mL)	4.97E+01	4.97E+01	4.97E+01
ESOL Solubility (mol/l)	2.22E-01	2.22E-01	2.22E-01
ESOL Class	Very soluble	Very soluble	Very soluble
Ali Log S	-2.02	-2.02	-2.02
Ali Solubility (mg/mL)	2.13E+00	2.13E+00	2.13E+00
Ali Solubility (mol/l)	9.49E-03	9.49E-03	9.49E-03
Ali Class	Soluble	Soluble	Soluble
Silicos-IT LogSw	-0.36	-0.36	-0.36
Silicos-IT Solubility (mg/mL)	9.83E+01	9.83E+01	9.83E+01
Silicos-IT Solubility (mol/l)	4.39E-01	4.39E-01	4.39E-01
Silicos-IT class	Soluble	Soluble	Soluble
GI absorption	Low	Low	Low
BBB permeant	No	No	No
Pgp substrate	No	No	No
CYP1A2 inhibitor	No	No	No
CYP2C19 inhibitor	No	No	No

CYP2C9 inhibitor	No	No	No
CYP2D6 inhibitor	No	No	No
CYP3A4 inhibitor	No	No	No
log Kp (cm/s)	-8.09	-8.09	-8.09
Lipinski #violations	0	0	0
Ghose #violations	1	1	1
Veber #violations	1	1	1
Egan #violations	1	1	1
Muegge #violations	1	1	1
Bioavailability Score	0.55	0.55	0.55
PAINS #alerts	0	0	0
Brenk #alerts	0	0	0
Leadlikeness #violations	1	1	1
Synthetic Accessibility	3.68	3.68	3.68

The bioavailability radar plots further illustrate the closely related physicochemical profiles of molecules **2a, 3a,** and **3b**. In all three cases, the radar diagrams show deviations from the optimal oral drug-like space, particularly along the polarity and solubility-related axes. Molecule 1 exhibits the most pronounced imbalance, with a strong shift toward high polarity and low lipophilicity, consistent with its elevated TPSA and multiple hydrogen-bond donors. Molecules **3a** and **3b** display more compact and balanced radar shapes, reflecting reduced polarity and slightly improved size and lipophilicity parameters, although they still fall partially outside the ideal region. Flexibility and saturation remain within acceptable ranges for all three compounds, indicating comparable conformational behavior. Overall, the radar analysis supports the numerical ADME data, highlighting excessive polarity as the primary limiting factor for oral bioavailability, while indicating that molecules **3a** and, especially, **3b** are closer to the desired physicochemical space and may be more suitable candidates for further optimization, as shown in Figure 1.

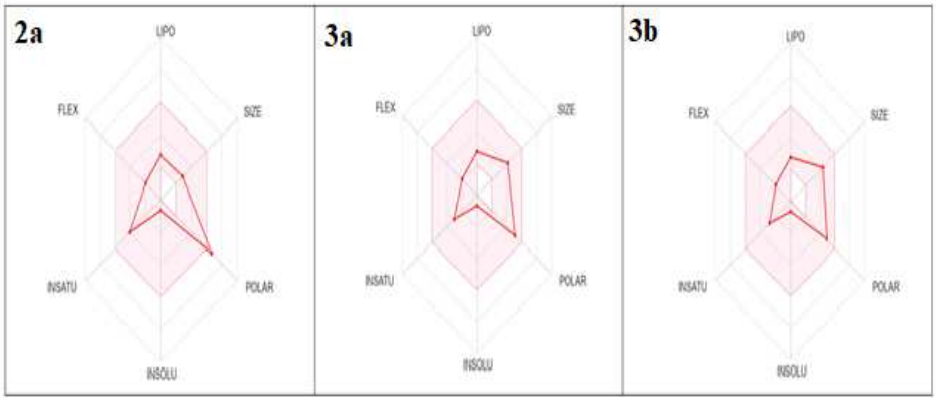


Figure 1. Radar charts showing pharmacokinetic parameters

The plot illustrated in Figure 2 shows the pharmacokinetic properties of molecules **2a, 3a,** and **3b** based on their WLOGP and TPSA values. All three compounds fall within the optimal regions for either blood–brain barrier (BBB) penetration or high human intestinal absorption (HIA). Molecule **2a** has a very high TPSA and low lipophilicity, placing it well outside both the BBB and HIA zones and

indicating poor permeability. Molecules **3a** and **3b** have moderately lower TPSA and higher WLOGP than molecule 2a but remain outside the favorable regions, suggesting limited oral absorption and no BBB penetration. Moreover, all compounds are predicted to be non-P-gp substrates, implying that efflux is not a limiting factor; rather, excessive polarity is the primary contributor to their poor permeability profiles.

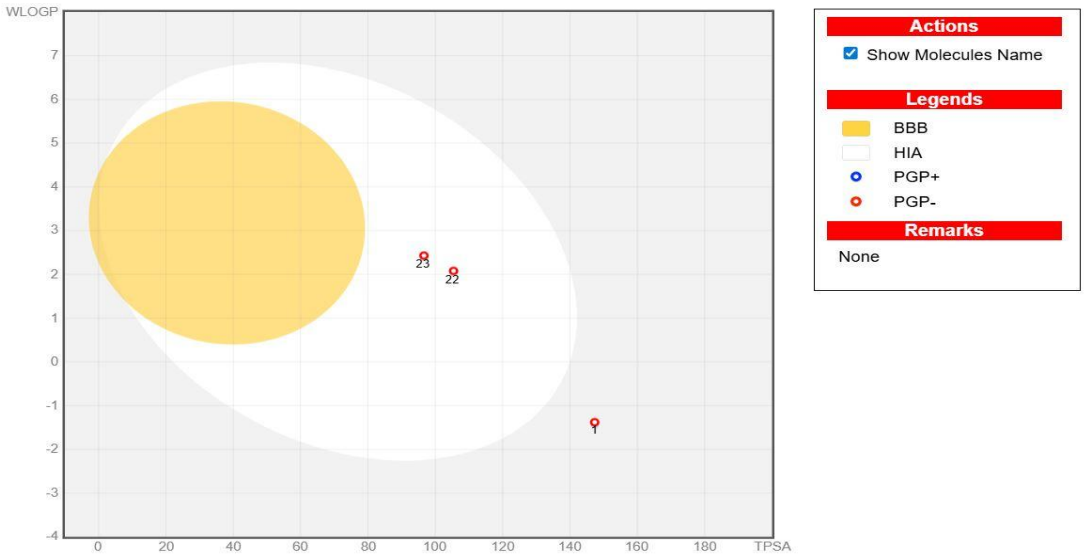


Figure 2. BOILED-Egg plot showing pharmacokinetic properties

Molecular docking analysis

Molecular docking is a crucial computational tool for determining interactions between ligands and proteins at the molecular level. In the current study, we aimed to predict the binding scores of synthesized derivatives with Trypanothione Reductase and N-Myristoyltransferase. Protozoan parasites of the genera Leishmania and Trypanosoma rely on specialized metabolic enzymes that are absent or markedly distinct from those of their mammalian hosts, making them attractive targets for antiparasitic drug development. Two such enzymes are trypanothione reductase and N-myristoyltransferase.

Trypanothione reductase is an NADPH-dependent flavoenzyme that maintains the intracellular redox balance of trypanosomatids by reducing trypanothione disulfide to its dithiol form. This reaction sustains the parasite's antioxidant defenses and protects against reactive oxygen species generated by the host immune system. Structural analysis of TR reveals a homodimeric FAD-containing enzyme with active-site residues that facilitate hydride transfer from NADPH to the disulfide substrate. Because mammals employ glutathione reductase rather than trypanothione reductase, TR represents a selective and validated chemotherapeutic target [46].

In contrast, N-myristoyltransferase catalyzes the covalent transfer of a myristoyl group from myristoyl-CoA to the N-terminal glycine of substrate proteins, a modification essential for protein–membrane association, signal transduction, and subcellular localization. The crystal structure of Leishmania

donovani elucidates the binding modes of myristoyl-CoA and peptide substrates, providing a template for the design of structure-guided inhibitors. Inhibition of NMT disrupts multiple vital cellular pathways, leading to parasite death [47].

Notably, the interaction of compounds **3a** and **3b** within the active site of N-Myristoyltransferase demonstrated notable binding affinities, with binding energies of -8.2 and -8.4 kcal/mol, respectively, as given in Table 3.

Table 4: Molecular docking scores of compounds **2a, 3a,** and **3b** in Trypanothione Reductase and N-Myristoyltransferase

Protein	Ligand Codes	Binding energy Kcal/mol	Hydrogen bond-forming residues	Hydrophobic interaction residues
2jk6 Trypanothione Reductase	**2a**	-5.9	MET333, TYR198, THR335	CYS57
	3a	-7.7	TYR198	CYS57, LYS60, ALA365
	3b	-7.0	THR335, LYS60	ALA365, LEU334, CYS57
2wuu N-Myristoyl-transferase	**2a**	-7.0	TYR345	TYR217, PHE232
	3a	-8.2	TYR345, SER330, PHE90	PHE232, TYR217
	3b	-8.4	TYR217, ASN376, TYR345	VAL81

Figures 3 and 4 provide a detailed representation of the two-dimensional and three-dimensional binding interactions between the studied compounds and the target enzyme, N-Myristoyltransferase. The binding analysis shows that several key amino acid residues stabilize the ligand-enzyme complex. Notably, TYR217, ASN376, and TYR345 are involved in the formation of hydrogen bonds, which contribute significantly to the binding affinity and specificity of the compounds. Additionally, VAL81 participates in alkyl interactions, further supporting the molecular stability within the binding pocket. These interactions suggest favorable, specific binding of the compounds to the active site of N-Myristoyltransferase, supporting their potential as inhibitors.

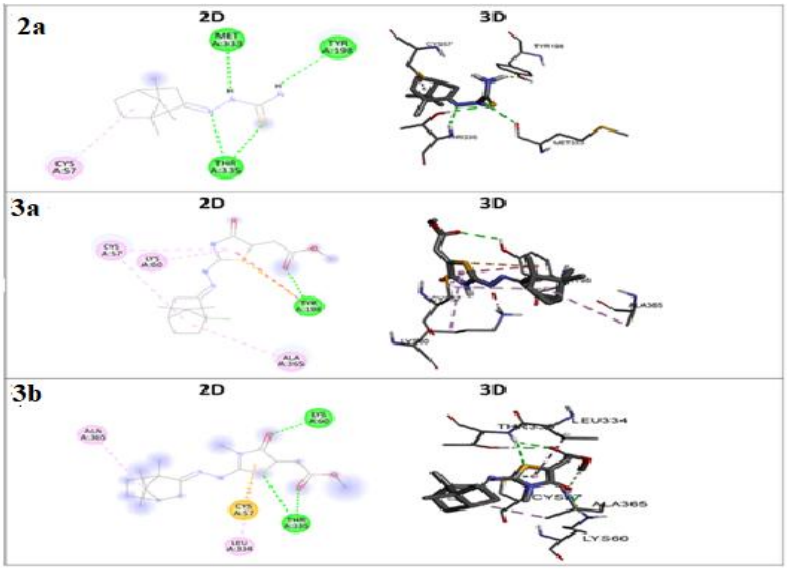


Figure 3. The predicted 2D and 3D binding pose*s* of compounds **2a, 3a,** and **3b** against Trypanothione Reductase.

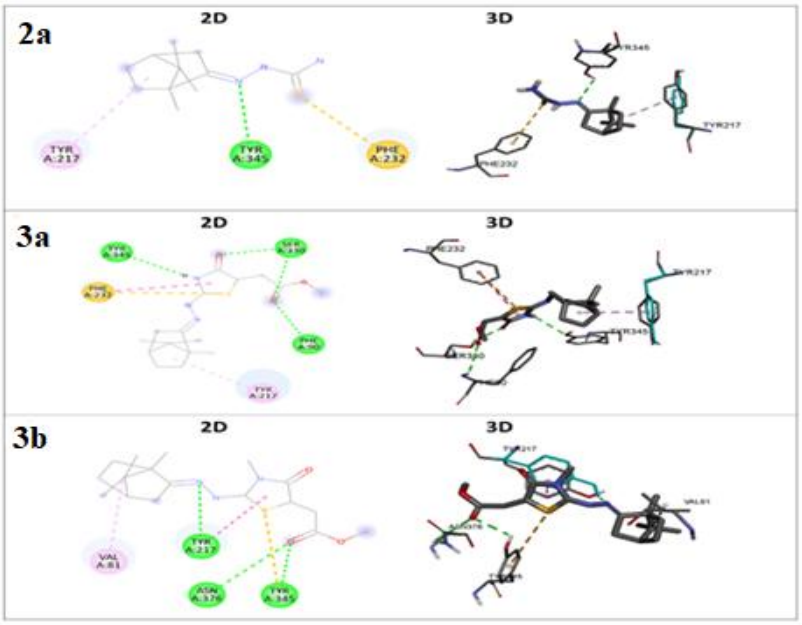


Figure 4. The predicted 2D and 3D binding pose*s* of compounds **2a, 3a,** and **3b** against N-Myristoyltransferase.

Density Functional Theory (DFT)

The quantum chemical properties of compounds **2a, 3a,** and **3b** provide insights into their electronic behavior and reactivity. Compound **3b** shows the lowest energy gap (ΔeV = 4.00), followed closely by compound **3a** (4.109eV), indicating their higher chemical reactivity and potential for electron transfer compared to compound 2a, which has a slightly larger gap (5.115 eV). All compounds have comparable dipole moments around 4.5 D, suggesting similar polarity, while compound **3b** exhibits the highest polarizability (251.647 α), implying a greater ability to respond to external electric fields. In general, polarizability increases with molecular size because larger molecules possess more electrons and a more easily distortable electron cloud (Figure 5*)*. Accordingly, species with greater molecular volume exhibit higher polarizability values, as evident from Tables 1 and 3. Optimization energies indicate that compound **2a** is the least stable (–992.842), whereas compounds **3a** and **3b** show greater thermodynamic stability. Overall, compound **3b** stands out with the highest polarizability and lowest energy gap, making it potentially more reactive and electronically adaptable, as given in Table 5.

Table 5: DFT parameters of compounds **2a, 3a,** and **3b**.

Codes	Optimization Energy	Dipole moment	Polarizability (α)	LUMO (hartree)	HOMO (hartree)	LUMO - HOMO (ΔeV)
2a	-992.842	4.640	146.411	-0.011	-0.199	5.115
3a	-1410.090	4.493	237.139	-0.084	-0.235	4.109
3b	-1449.382	4.7042	251.647	-0.082	-0.229	4.000

*** 1 Hartree=27.2114 eV**

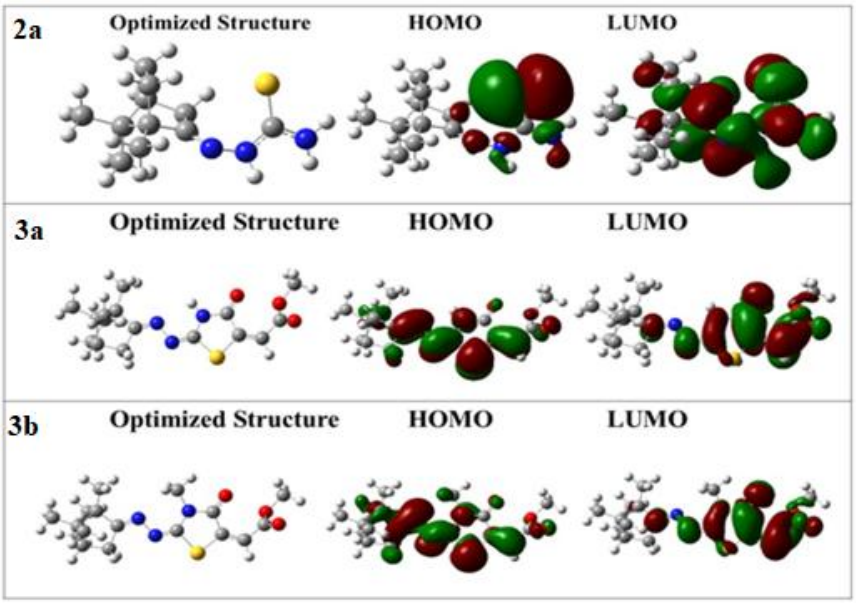


Figure 5. Optimized geometries and HOMO-LUMO orbitals of compounds **2a, 3a,** and **3b**.

Chemical reactivity parameters

The chemical reactivity descriptors of compounds **2a, 3a,** and **3b** offer valuable insights into their electronic behavior and potential biological activity. Compound **3b** exhibits the highest softness (6.803 eV^{-1}) and the lowest hardness (0.074 eV), suggesting it is the most chemically reactive and easily polarizable among the three. Similarly, compounds **3a** and **3b** show higher electrophilicity indices (0.168 and 0.164 eV, respectively) compared to compound **2a** (0.059 eV), indicating a greater ability to accept electrons, which is favorable in electrophilic interactions. The chemical potential (μ) and electronegativity (χ) follow the same trend, being higher in compounds **3a** and **3b**. Overall, compounds **3a** and **3b** display superior electrophilic nature, softness, and reactivity, making them more promising candidates for further biological or pharmacological evaluation (Table 5).

Table 5. An overview of the Chemical Reactivity Descriptors for **2a, 3a,** and **3b**

Codes	Chemical Potential μ (eV)	Electronegativity X (eV)	Hardness η (eV)	softness S (eV^{-1})	Electrophilicity Index ω (eV)
2a	-0.105	0.105	0.094	5.328	0.059
3a	-0.159	0.159	0.076	6.605	0.168
3b	-0.156	0.156	0.074	6.803	0.164

Conclusion

In conclusion, we have presented a straightforward synthesis of thiosemicarbazone and thiazolidinone derivatives derived from (R)-camphor precursors, thereby extending our previous work. The structures of the synthesized compounds were confirmed using NMR spectroscopy (^{1}H and ^{13}C) and high-resolution mass spectrometry (HRMS). Structural parameters were further analyzed using DFT calculations at the B3LYP/6-311++G(d,p) level. The intramolecular charge transfer interactions were supported by the calculated HOMO–LUMO energy gap values. The compounds were biologically

evaluated for their *in vitro* antiparasitic activity, demonstrating efficacy against Leishmania major (both promastigote and amastigote forms) as well as Toxoplasma gondii tachyzoites. Docking calculations predicted favorable interactions of selected compounds **2a, 3a,** and **3b** with the active sites of trypanothione reductase and N-myristoyltransferase, providing structural hypotheses that warrant experimental validation. These results suggest favorable predicted binding affinities and suitable molecular fitting of the compounds within the enzyme active sites.

Declarations

Ethics approval and consent

The laboratory animals were handled and reared according to the guidelines and regulations of the Committee of Research Ethics, Deanship of Scientific Research, Qassim University, as indicated by permission number 20-03-20.

Competing interests

The authors declare no competing interests.

Finding

The authors received funding for this work (project number VPMA4/2022/07).

Conflict of interest:

The authors declare that there are no conflicts of interest.

Disclosure statement

No potential conflict of interest was reported by the authors.

Data Availability Statement

The data supporting the findings of this study are available within the article and its Supplementary Materials.

Supplementary data

To view the supplementary data that accompany this paper, please visit the journal website.

Acknowledgments

The authors would like to thank the Deanship of Graduate Studies and Scientific Research at Qassim University for financial support (QU-APC-2026). The authors gratefully acknowledge the financial support provided by Cadi Ayyad University and the CNRST through the VPMA4 (Valorisation of Medicinal and Aromatic Plants 4th edition) program.

References

[1] R.G. Wamai, J. Kahn, J. McGloin, G. Ziaggi, Visceral leishmaniasis: a global overview, Journal of Global Health Science. 2 (2020). https://doi.org/10.35500/jghs.2020.2.e3.

[2] P. Cecílio, A. Cordeiro-da-Silva, F. Oliveira, Sand flies: Basic information on the vectors of leishmaniasis and their interactions with Leishmania parasites, Communications Biology. 5 (2022) 305. https://doi.org/10.1038/s42003-022-03240-z.

[3] S. Arumugam, B.M. Scorza, C. Petersen, Visceral Leishmaniasis and the Skin: Dermal Parasite Transmission to Sand Flies, Pathogens. 11 (2022) 610. https://doi.org/10.3390/pathogens11060610.

[4] E. Torres-Guerrero, M.R. Quintanilla-Cedillo, J. Ruiz-Esmenjaud, R. Arenas, Leishmaniasis: a review, F1000Research. 6 (2017) 750. https://doi.org/10.12688/f1000research.11120.1.

[5] N.M. Bemben, M.L. Berg, Efficacy of inactivated vaccines in patients treated with immunosuppressive drug therapy, Pharmacotherapy: The Journal of Human Pharmacology and Drug Therapy. 42 (2022) 334–342. https://doi.org/10.1002/phar.2671.

[6] H. Zhang, R. Yan, Y. Liu, M. Yu, Z. He, J. Xiao, K. Li, G. Liu, Q. Ning, Y. Li, Progress in antileishmanial drugs: Mechanisms, challenges, and prospects, PLOS Neglected Tropical Diseases. 19 (2025) e0012735. https://doi.org/10.1371/journal.pntd.0012735.

[7] S. Pradhan, R.A. Schwartz, A. Patil, S. Grabbe, M. Goldust, Treatment options for leishmaniasis, Clinical and Experimental Dermatology. 47 (2022) 516–521. https://doi.org/10.1111/ced.14919.

[8] M. Soni, J.V. Pratap, Development of Novel Anti-Leishmanials: The Case for Structure-Based Approaches, Pathogens. 11 (2022) 950. https://doi.org/10.3390/pathogens11080950.

[9] T. Masne, D. Kumar, D. Bansode, A review of leishmaniasis: current knowledge and future directions of heterocyclic molecules, Exploration of Drug Science. (2024) 508–539. https://doi.org/10.37349/eds.2024.00059.

[10] M. Abirami, B. Karan Kumar, Faheem, S. Dey, S. Johri, R.M. Reguera, R. Balaña-Fouce, K.V. Gowri Chandra Sekhar, M. Sankaranarayanan, Molecular-level strategic goals and repressors in Leishmaniasis – Integrated data to accelerate target-based heterocyclic scaffolds, European Journal of Medicinal Chemistry. 257 (2023) 115471. https://doi.org/10.1016/j.ejmech.2023.115471.

[11] M. Fawzi, A. Bimoussa, Y. Laamari, A.N. Oussidi, A. Oubella, E.M. Ketatni, M. Saadi, L. El Ammari, H. Morjani, M.Y. Ait Itto, A. Auhmani, New (S)-verbenone-isoxazoline-1,3,4-thiadiazole Hybrids: Synthesis, Anticancer Activity and Apoptosis-Inducing Effect, Future Medicinal Chemistry. 15 (2023) 1603–1619. https://doi.org/10.4155/fmc-2023-0173.

[12] E. Kabir, M. Uzzaman, A review on biological and medicinal impact of heterocyclic compounds, Results in Chemistry. 4 (2022) 100606. https://doi.org/10.1016/j.rechem.2022.100606.

[13] B.A. Federici, Pathogens of Insects, in: Encyclopedia of Insects, Elsevier, 2009: pp. 757–765. https://doi.org/10.1016/B978-0-12-374144-8.00202-2.

[14] R. Pal, G. Teli, M.J. Akhtar, G.S.P. Matada, The role of natural anti-parasitic guided development of synthetic drugs for leishmaniasis, European Journal of Medicinal Chemistry. 258 (2023) 115609. https://doi.org/10.1016/j.ejmech.2023.115609.

[15] S. Hu, Z. Batool, X. Zheng, Y. Yang, A. Ullah, B. Shen, Exploration of innovative drug repurposing strategies for combating human protozoan diseases: Advances, challenges, and opportunities, Journal of Pharmaceutical Analysis. 15 (2025) 101084. https://doi.org/10.1016/j.jpha.2024.101084.

[16] A. Boualli, Y. Laamari, A. Bimoussa, S.A. Ejaz, H.M. Attaullah, A. Riahi, A. Robert, J. Daran, I.S. Al Nasr, W.S. Koko, T.A. Khan, B. Biersack, A. Auhmani, M.Y.A. Itto, Design, Hemisynthesis, Characterization, Molecular Docking, and Dynamics Evaluation of Novel Totarol-1,2,3-Triazole Derivatives as Leishmaniasis and Toxoplasmosis Agents, Chemical Biology & Drug Design. 105 (2025). https://doi.org/10.1111/cbdd.70042.

[17] A. Bimoussa, A.N. Ait, O. Mourad, F.A. El, M. Yassine, Potential Anticancer Agents Based on Monoterpenic Skeleton With Mono and Bis- - Isoxazoline Derivatives : Diastereoselective Synthesis , Experimental Study , Evaluation of Biological Activity , and Molecular Docking, Journal of Heterocyclic Chemistry RESEARCH. (2026) 1–17. https://doi.org/10.1002/jhet.70158.

[18] L.R.P. de Siqueira, P.A.T. de Moraes Gomes, L.P. de Lima Ferreira, M.J.B. de Melo Rêgo, A.C.L. Leite, Multi-target compounds acting in cancer progression: Focus on thiosemicarbazone, thiazole and thiazolidinone analogues, European Journal of Medicinal Chemistry. 170 (2019) 237–260. https://doi.org/10.1016/j.ejmech.2019.03.024.

[19] K. Kouchkar, Y. Boumedjane, D. Harkati, M. Mogren Al-Mogren, M. Hochlaf, Ab initio structural study of 2-imino-4-thiazolidinone derivatives and their anti-proliferative activity against A549 and H460 human lung carcinoma cells, Computational and Theoretical Chemistry. 1228 (2023) 114279. https://doi.org/10.1016/j.comptc.2023.114279.

[20] A. Bimoussa, M. Fawzi, A. Oubella, S.A. Ejaz, M. Sajjad Bilal, M. Labd Taha, A. Auhmani, H. Morjani, A. Robert, A. Riahi, M.Y. Ait Itto, Hybrids of thiazolidinone with 1,2,3-triazole derivatives: design, synthesis, biological evaluation, in silico studies, molecular docking, molecular dynamics simulations, and ADMET profiling, Journal of Biomolecular Structure and Dynamics. 41 (2023) 11987–11999. https://doi.org/10.1080/07391102.2022.2164357.

[21] A. Bimoussa, A. Oubella, Y. Laamari, M. Fawzi, M.E. Hachim, M.Y. Ait Itto, H. Morjani, E.M. Ketatni, O. Mentre, A. Auhmani, Hybrid of the 1,2,3-triazole nucleus and sesquiterpene skeleton as a potential antitumor agent: Hemisynthesis, molecular structure, Hirshfeld surface analysis, density functional theory, and in vitro cytotoxic and apoptotic effects, Journal of Heterocyclic Chemistry. 58 (2021) 2334–2347. https://doi.org/10.1002/jhet.4359.

[22] A. Bimoussa, A. Oubella, M.A. Alossaimi, M. Aziz, H.M. Attaullah, S.A. Ejaz, H. Morjani, A. Auhmani, A. Robert, A. Riahi, Y. Riadi, M.Y. Ait Itto, Novel Bis-1,2,3-triazole-thiazolidinone hybrid as anticancer agents that induce apoptosis and molecular modeling study, Future Medicinal Chemistry. 16 (2024) 2193–2210. https://doi.org/10.1080/17568919.2024.2394019.

[23] R. Matsa, P. Makam, M. Kaushik, S.L. Hoti, T. Kannan, Thiosemicarbazone derivatives: Design, synthesis and in vitro antimalarial activity studies, European Journal of Pharmaceutical Sciences. 137 (2019) 104986. https://doi.org/10.1016/j.ejps.2019.104986.

[24] R. Singh, J. Sindhu, P. Kumar, M. Hooda, R. Aggarwal, S. Lal, S. Ahmadi, S. Lotfi, D. Singh, H. Kumar, α-Amylase Inhibitors Based on Thiazolidinone Skeleton: A Promising Approach in Diabetes Management, ChemistrySelect. 8 (2023). https://doi.org/10.1002/slct.202303852.

[25] W.I. El-Sofany, E.M.S. Azzam, S. Latif, K. Hamden, Spirothiazolidine-Derivative on Silver Nanoparticles and Carbon Nanotubes: Evaluation of Antibacterial, Anti-Fungal, Anti-Inflammatory, Antioxidant and Gastroprotective Activities, Pharmaceutics. 16 (2024) 901. https://doi.org/10.3390/pharmaceutics16070901.

[26] R. Rajalakshmi, S. Ramkumar, Synthesis and Biological Applications of Thiazolidinone, in: Strategies for the Synthesis of Heterocycles and Their Applications, IntechOpen, 2023. https://doi.org/10.5772/intechopen.109102.

[27] T.S. Chitre, S.M. Patil, A.G. Sujalegaonkar, K.D. Asgaonkar, Designing of Thiazolidin-4-one Pharmacophore using QSAR Studies for Anti-HIV Activity, Indian Journal of Pharmaceutical Education and Research. 55 (2021) 581–589. https://doi.org/10.5530/ijper.55.2.97.

[28] R.A.K. Alharbi, S.M. Riyadh, N.S. Al-Kaff, M.A. Said, Newly synthesized Bis-Hydrazono[1,3,4] thiadiazoles as Anti-Alzheimer's Agents: Greener past and In-Vitro acetylcholinesterase inhibition assay investigations, Journal of Saudi Chemical Society. 28 (2024) 101868. https://doi.org/10.1016/j.jscs.2024.101868.

[29] C. Tratrat, Novel Thiazole-Based Thiazolidinones as Potent Anti-infective Agents: In silico PASS and Toxicity Prediction, Synthesis, Biological Evaluation and Molecular Modelling, Combinatorial Chemistry & High Throughput Screening. 23 (2020) 126–140. https://doi.org/10.2174/1386207323666200127115238.

[30] R.R. de O. Silva, P.A. Meira, C.A. Merfels, M.S.A. Palma, Improvements to the Pioglitazone synthetic route using microreactor technology and aspects of green chemistry, Chemical Engineering Research and Design. 218 (2025) 697–706. https://doi.org/10.1016/j.cherd.2025.05.002.

[31] S. Mandal, D.S. Chiriki, B.M. Gurupadayya, I.A. Chethan, B.R. Prashantha Kumar, Phenyl glycine incorporated glitazones as promising novel antidiabetic agents through PPARγ agonism: Design, synthesis and preclinical studies, European Journal of Medicinal Chemistry Reports. 6 (2022) 100067. https://doi.org/10.1016/j.ejmcr.2022.100067.

[32] A. Bimoussa, A. Oubella, I. Bjij, M. Fawzi, Y. Laamari, M.Y. Ait Itto, A. Auhmani, H. Morjani, D. Cherqaoui, A. Auhmani, Design, Synthesis, Biological and Computational Assessment of New Thiazolidin-4-one Derivatives as Potential Anticancer Agents Through the Apoptosis Pathway, ChemistrySelect. 7 (2022) 1–11. https://doi.org/10.1002/slct.202200165.

[33] A. N'ait Ousidi, M.Y. Ait Itto, A. Auhmani, A. Riahi, A. Robert, A. Auhmani, J.-C. Daran, New polysubstituted monoterpenic thiazolidinones: synthesis, spectroscopic and crystal structure studies, Acta Crystallographica Section C Structural Chemistry. 74 (2018) 1629–1634. https://doi.org/10.1107/S2053229618015802.

[34] A. Ousidi, M. Youssef Ait Itto, A. Auhmani, M. Barakate, A. Riahi, H. Ben El Ayouchia, H. Anane, N. El Aouad, M. De La Cruz, C. Díaz, Synthesis, theoretical and biological studies of some novel Monoterpenic thiazolidin-4-ones, IOSR Journal of Applied Chemistry (IOSR-JAC. 9 (2016) 52–61. https://doi.org/10.9790/5736-0911025261.

[35] I.S. Al Nasr, A. Corona, W.S. Koko, T.A. Khan, R. Ben Said, I. Daoud, S. Rahali, E. Tramontano, R. Schobert, N. Amdouni, B. Biersack, Versatile anti-infective properties of pyrido- and dihydropyrido[2,3-d]pyrimidine-based compounds, Bioorganic & Medicinal Chemistry. 90 (2023) 117376.

https://doi.org/10.1016/j.bmc.2023.117376.
[36] A. Daina, V. Zoete, Application of the swissdrugdesign online resources in virtual screening, International Journal of Molecular Sciences. 20 (2019) 4612. https://doi.org/10.3390/ijms20184612.
[37] C.-Y. Jia, J.-Y. Li, G.-F. Hao, G.-F. Yang, A drug-likeness toolbox facilitates ADMET study in drug discovery, Drug Discovery Today. 25 (2020) 248–258. https://doi.org/10.1016/j.drudis.2019.10.014.
[38] C.A. Lipinski, F. Lombardo, B.W. Dominy, P.J. Feeney, Experimental and computational approaches to estimate solubility and permeability in drug discovery and development settings, Advanced Drug Delivery Reviews. 64 (2012) 4–17. https://doi.org/10.1016/j.addr.2012.09.019.
[39] D.S. Goodsell, M.F. Sanner, A.J. Olson, S. Forli, The <scp>AutoDock</scp> suite at 30, Protein Science. 30 (2021) 31–43. https://doi.org/10.1002/pro.3934.
[40] T. Brown, NSTA's NEW Multi-Touch Books Now Available on the iBookstore !, (2014) 71–73.
[41] A. Bimoussa, M.E. Hachim, Y. Laamari, M.H. Geesi, M.T. Muhammed, M.A. Alamri, Y. Riadi, I. Yildiz, A. Oubella, S.H. Alotaibi, A. Auhmani, M.Y.A. Itto, Computational assessment of the reactivity and anticancer activity of 1,2,3-triazole-thiazolidinones derivatives: An approach combining DFT calculations, molecular dynamics simulations, molecular docking, and ADMET, Journal of Molecular Structure. 1321 (2025) 139756. https://doi.org/10.1016/j.molstruc.2024.139756.
[42] M.D. Hanwell, D.E. Curtis, D.C. Lonie, T. Vandermeersch, E. Zurek, G.R. Hutchison, Avogadro: an advanced semantic chemical editor, visualization, and analysis platform, Journal of Cheminformatics. 4 (2012) 17. https://doi.org/10.1186/1758-2946-4-17.
[43] U. Vanitha, R. Elancheran, V. Manikandan, S. Kabilan, K. Krishnasamy, Design, synthesis, characterization, molecular docking and computational studies of 3-phenyl-2-thioxoimidazolidin-4-one derivatives, Journal of Molecular Structure. 1246 (2021) 131212. https://doi.org/10.1016/j.molstruc.2021.131212.
[44] A.N. Ousidi, A. Bimoussa, M. Loubidi, M. Fawzi, Y. Laamari, A. Oubella, M. Maatallah, S. Berteina-Raboin, A. Auhmani, M.L. Taha, H. Morjani, M.Y. Ait Itto, Design, Synthesis, Cytotoxic Effect Evaluation and Molecular Docking of (R)-Camphor-Based Thiazolidinone-Isoxazole and Thiazolidinone-1,2,3-triazole Hybrids", ChemistrySelect. 8 (2023). https://doi.org/10.1002/slct.202203349.
[45] J.C. N'ait Ousidi, Abdellah Ait Itto, Moulay Youssef Auhmani, Aziz Riahi, Abdelkhalek Robert, Anthony Auhmani, Abdelwahed Daran, New polysubstituted monoterpenic thiazolidinones: synthesis, spectroscopic and crystal structure studies, Acta Crystallographica Section C: Structural Chemistry. 74 (2018) 1629–1634. https://doi.org/10.1107/S2053229618015802.
[46] T. Battista, G. Colotti, A. Ilari, A. Fiorillo, Targeting Trypanothione Reductase, a Key Enzyme in the Redox Trypanosomatid Metabolism, to Develop New Drugs against Leishmaniasis and Trypanosomiases, Molecules. 25 (2020) 1924. https://doi.org/10.3390/molecules25081924.
[47] E.W. TATE, A.S. BELL, M.D. RACKHAM, M.H. WRIGHT, N- Myristoyltransferase as a potential drug target in malaria and leishmaniasis, Parasitology. 141 (2014) 37–49. https://doi.org/10.1017/S0031182013000450.

Supplementary Files

This is a list of supplementary files associated with this preprint. Click to download.

- Supplementaryinformation.docx